An inversion-based deblending solution

Amarjeet Kumar, Gary Hampson, Neil Vice and Troy Thompson, DownUnder GeoSolutions, Perth, Australia*

SUMMARY

Blended seismic acquisition is an efficient method of surveying that can considerably reduce the cost of high-density surveys. The method results in overlapping records, analogous to seismic interference, that must be separated prior to subsequent processing. When a shot is fired on top of weak signal from an earlier shot, recovery of that signal is a well-known, significant challenge. We have designed a novel iterative-relaxation inversion algorithm to slowly reconstruct the deblended shot records from the blended input. High-quality results were obtained using our algorithm on real marine streamer, ocean-bottom node and land datasets.

INTRODUCTION

So-called "blended" seismic data acquisition (e.g., Berkhout, 2008) has enjoyed increasing popularity recently because it has realised some of the potential economic and spatial sampling benefits it promised. However, actuations of seismic sources ("shots") that overlap in time currently need to be separated (deblended) so that they can be processed as if they had been acquired without overlap. When a shot is fired on top of weak signal from an earlier shot, recovery of that signal is a well-known, significant challenge. For example, Maraschini et al. (2016) proposed a two-step denoising process to maximise the preservation of signal using a robust rank reduction filter (Trickett et al., 2012). However, their results show that weak signal is still not recovered completely, especially at depth, and that the method suffers from denoising artefacts.

Hampson et al. (2008) note that the key observation in the source separation problem is that as long as the times between successive shots are suitably random the resulting source cross-talk will appear like unpredictable noise in the common-offset, -receiver and -midpoint domains. Inversion-type deblending methods (Akerberg et al., 2008; Moore et al., 2008; van Borselen et al., 2012) take advantage of sparse representations of predictable seismic signals. Other deblending techniques focus on iterative approaches (e.g., Abma, 2010; Mahdad et al., 2011; Beasley et al., 2012). There continues to be a need for improved methods to separate energy from interfering seismic sources. Here we describe a new inversion-based deblending algorithm that performs exceptionally well at recovering both the weaker and stronger parts of the wavefield without the strong denoising artefacts often seen in other deblending methods. It is based on an iterative thresholding algorithm. The effectiveness of the algorithm rests upon the novel manner in which the thresholding operation is performed and the manner in which the threshold is gently relaxed to finally reconstruct the shots as if they had been acquired separately. The results obtained on ocean-bottom node (OBN) and land field data show that the algorithm is very effective. Although not presented in this abstract, we experience equally effective results with marine streamer data.

METHOD

We denote blended seismic data as $\mathbf{d}(t,r,s)$, where t, r, and s represent time, receiver and source indices, respectively. Let $\mathbf{m}(t,r,s)$ represent the unblended seismic data. The blended seismic data ($\mathbf{d}$) can be written in the operator form,

$$\mathbf{d} = \mathbf{\Gamma m} \tag{1}$$

where $\mathbf{\Gamma}$ is a blending matrix. The blending matrix is entirely general, however, in this particular case, it contains the firing times of the individual seismic sources. Equation (1) is the forward blending model. The knowns are the blended shot-records ($\mathbf{d}$) and the blending matrix ($\mathbf{\Gamma}$). The unknowns are a set of deblended shot-records ($\mathbf{m}$) as if they had been acquired separately.

To retrieve individual deblended shot records ($\mathbf{m}$) from blended data ($\mathbf{d}$) using equation (1), an inversion has to be performed. This is an under-determined problem because $\mathbf{d}$ has fewer rows than $\mathbf{m}$. As a consequence, a direct inversion cannot be performed. If we re-blend the solution, we require it to fit the observed blended data. Therefore we define our data misfit to be the l_2 residual,

$$J = \|\mathbf{d} - \mathbf{\Gamma m}\|_2^2 . \tag{2}$$

To resolve the indeterminacy, constraints are required which reflect assumptions about the solution. We make the reasonable assumption that properly deblended data can be sparsely represented in a suitable transform domain. Therefore, we add a sparsity-promoting constraint term to the l_2 data misfit function (2) and solve the system as the basis pursuit l_p-analysis problem,

$$\tilde{\mathbf{m}} = \operatorname{argmin}\|\mathbf{Fm}\|_S \quad \text{s.t} \quad \mathbf{d} = \mathbf{\Gamma m}. \tag{3}$$

The estimate of the deblended output is denoted $\tilde{\mathbf{m}}$, $\mathbf{F}$ is any suitable sparsity-promoting transform and $\|.\|_S$ represents a sparse norm. Results shown in this paper use a windowed 3D Fourier transform. Minimizing the l_p -norm in equation (3) promotes sparsity in $\mathbf{Fm}$ while the equality constraint ensures that the re-blended solution matches the input data. Of the many methods available, we use an iterative thresholding procedure to solve equation (3). Our new thresholding iteration is,

$$\mathbf{m}^i = \left\lfloor \mathbf{m}^{i-1} + \alpha \mathbf{\Gamma}^H \left(\mathbf{d} - \Lambda \mathbf{\Gamma m}^{i-1} \right) \right\rfloor \tag{4}$$

where i is iteration number and α is the step length. The operator $\lfloor . \rfloor$ indicates a thresholding operator and Λ denotes time range selection. The success of our algorithm comes from this thresholding operation, where the threshold is gently relaxed over many iterations to finally reconstruct the deblended shots. Our objective is to explain all of the input data as a blending of the deblended shot records, that is, we iterate equation (4) until the residual is negligible.

10.1190/segam2020-3427002.1

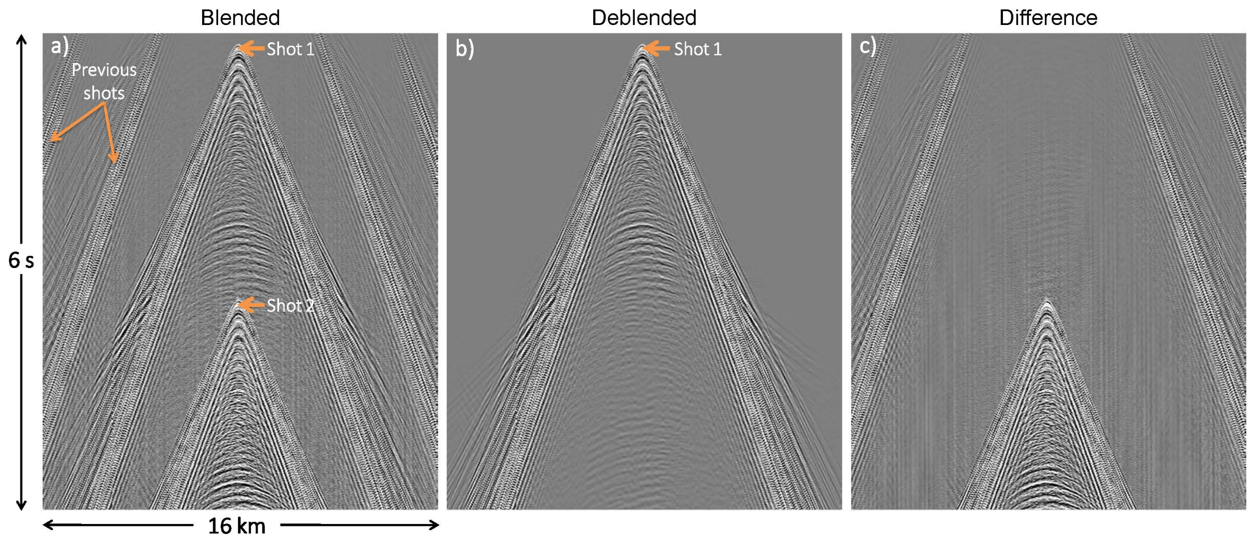

Figure 1: A shot record from an OBN survey when one source vessel (with a triple-source configuration) was active: a) input data before deblending; b) deblended output; c) difference between a) and b). (Data courtesy of AGS and TGS)

EXAMPLES

We first show real OBN data examples from the North Sea. The acquisition was carried out using initially two (and later three) source vessels (each with a triple-source configuration) firing independently into continuously recording nodes. For the northern part of the survey, a number of the shots were acquired with just a single vessel active. Figure 1a shows an example of a blended shot record from this part of the survey. The deblended result and the difference between blended and deblended data are shown in Figures 1b and c, respectively. The result demonstrates that the primary shot has been successfully reconstructed, and the difference panel does not show any sign of primary leakage. This is a good example of strong interference being successfully removed to reveal weak underlying signal.

In a different part of the survey, the deblending problem was more complex because at least two other seismic contractors were shooting surveys nearby at the same time. Figure 2 depicts the case where one particular survey was in very close proximity and was firing directly over the OBN receiver spread. Consequently, very strong seismic interference (SI) was also unintentionally blended with the planned shots from the triple-source vessels. At one stage during the survey 14 sources were being fired in the vicinity of the nodes. The seismic interference was included as part of the deblending problem using the shot times of the interfering sources which were provided by the other contractors. The data was deblended with and without using the shot times from the interfering surveys (shown in Figure 3). Figure 3a shows the input blended shot record; Figure 3b shows the deblended result without using the SI shot times; Figure 3c shows the deblended result which included the SI shot times. SI shots are indicated by white arrows. Comparing Figures 3b and 3c, it can be seen that the SI shots are perfectly removed. The SI shots are not only cleanly separated but the weak reflections, critical for AVO analysis, are also nicely recovered. These results show that seismic interference is simply an unintended form of blended acquisition and that our deblending algorithm provides an elegant solution.

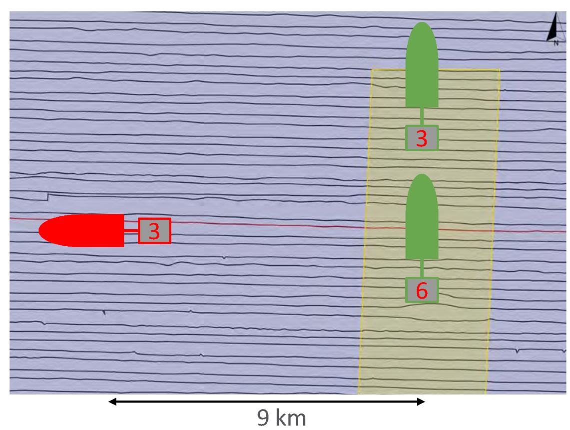

Figure 2: A map illustrating the proximity of two source vessels (green) from a nearby survey. These vessels were firing directly over the OBN receiver spread (shown by the black lines) with a total of 9 sources. An active OBN source vessel (a triple-source configuration) is depicted in red.

The southern part of the survey was shot with three source vessels. The next example is taken from the time when three vessels were shooting simultaneously within 15 km of each other (Figure 4a). Again, the deblended result and the difference panel (Figures 4b and c) show that the algorithm is very robust in separating the blended signal even in the case of multiple source vessels.

Figure 5 shows a real land data example from a 3D broadband

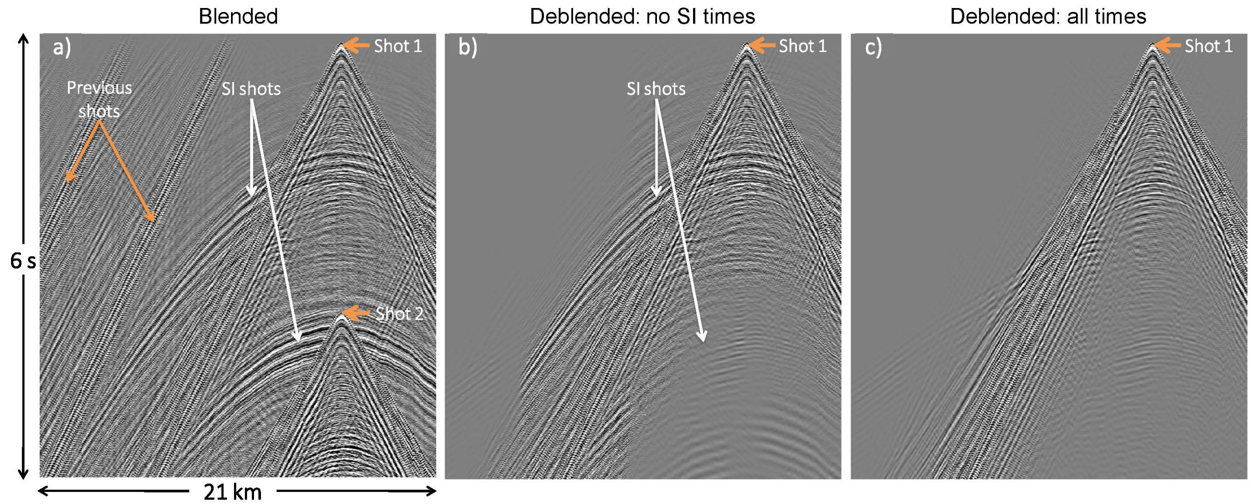

Figure 3: A shot record from an OBN survey showing seismic interference (SI) from a nearby survey: a) input data before deblending; b) deblended output without using the SI shot times from the interfering survey; c) deblended output using the SI shot times from the interfering survey. (Data courtesy of AGS and TGS)

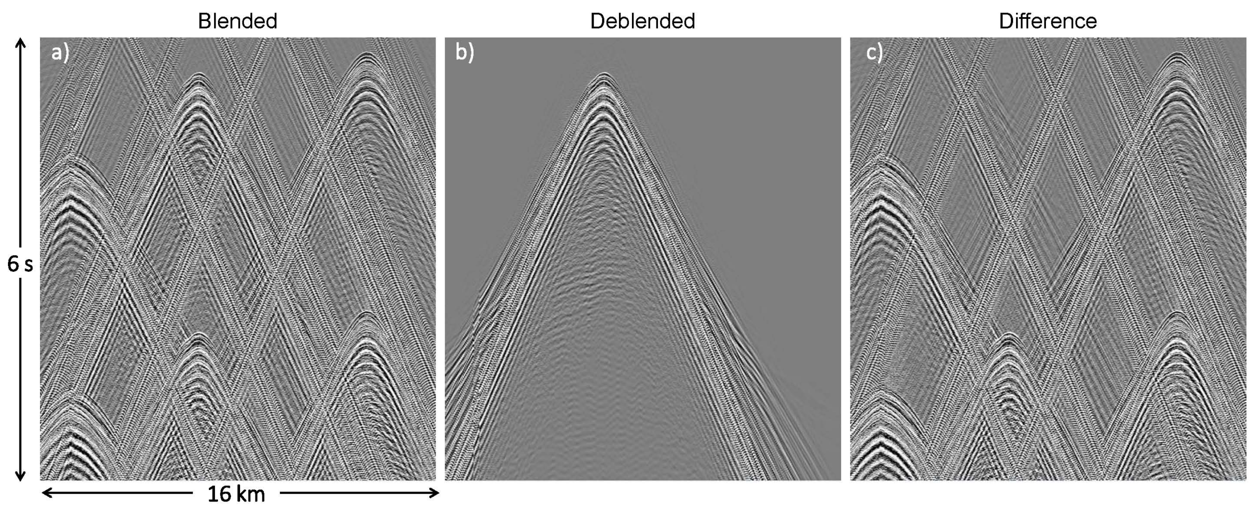

Figure 4: A shot record from an OBN survey when three source vessels (each with a triple-source configuration) were active: a) input data before deblending; b) deblended output; c) difference between a) and b). (Data courtesy of AGS and TGS)

survey onshore Egypt (after Yanchak et al., 2019). The basic 3D survey geometry consisted of 40 lines of receivers at 12.5 m intervals separated by 125 m. The source lines were perpendicular, also with a separation of 125 m, and a source interval of 12.5 m. Up to 30 Vibroseis units were operational at any one time.

In order to help evaluate the deblending performance, one of the production source lines was reacquired with only a pair of Vibroseis units performing in "flip/flop" mode to ensure that there was no interference between shot records. Therefore, for that particular source line, a perfect deblending result (non-blended data) was available as a benchmark. We tested our method to deblend this data and the result is shown in Figure 5b. Comparing our result with non-blended data (Figure 5c), it is almost indistinguishable.

It is important to inspect the low frequency components after separation. A cross-spread time slice of the input data, deblended output and non-blended data are shown in Figure 6 after a 6 Hz high-cut filter (after Yanchak et al., 2019). It can be observed that our results are not compromised with respect to low frequency components of the deblended data, and it matches perfectly with the non-blended data. Our results in Figures 5b and 6b are arguably better than the non-blended data (Figures 5c and 6c) due to the increase in SNR that comes naturally from inversion-based deblending (Beasley et al., 2012). Due to limited space we have not shown any marine streamer examples in this abstract. However, in our presentation we shall show, as in our earlier publication (Kumar et al., 2020),

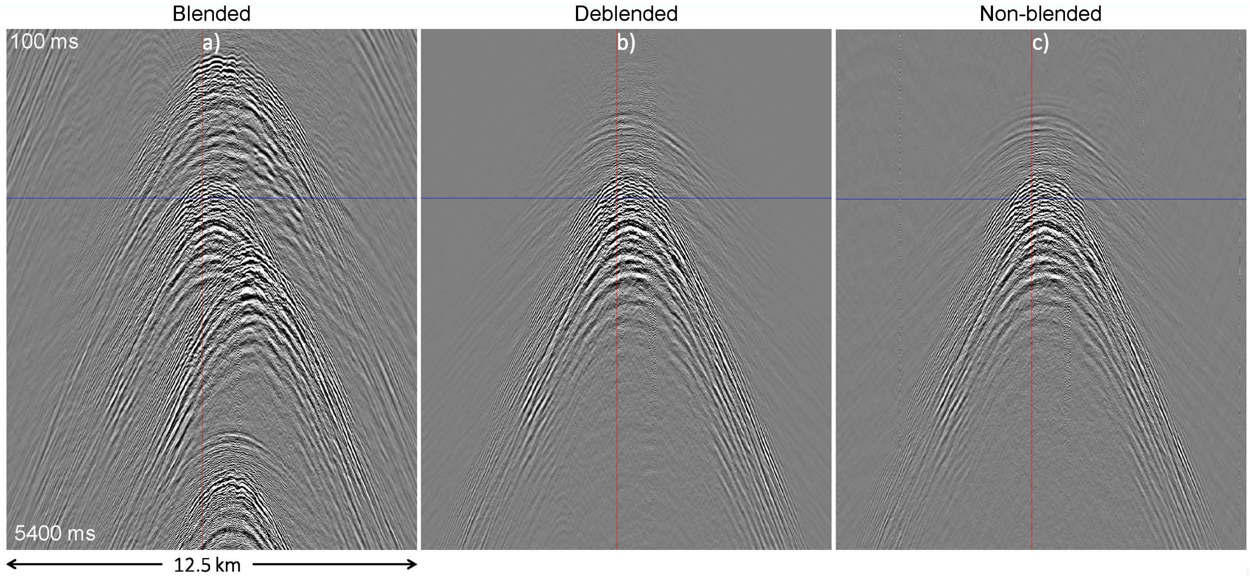

Figure 5: A shot record from a 3D land survey: a) input data before deblending; b) deblended output; c) non-blended data representative of a perfect deblending result. (Data courtesy of Apache)

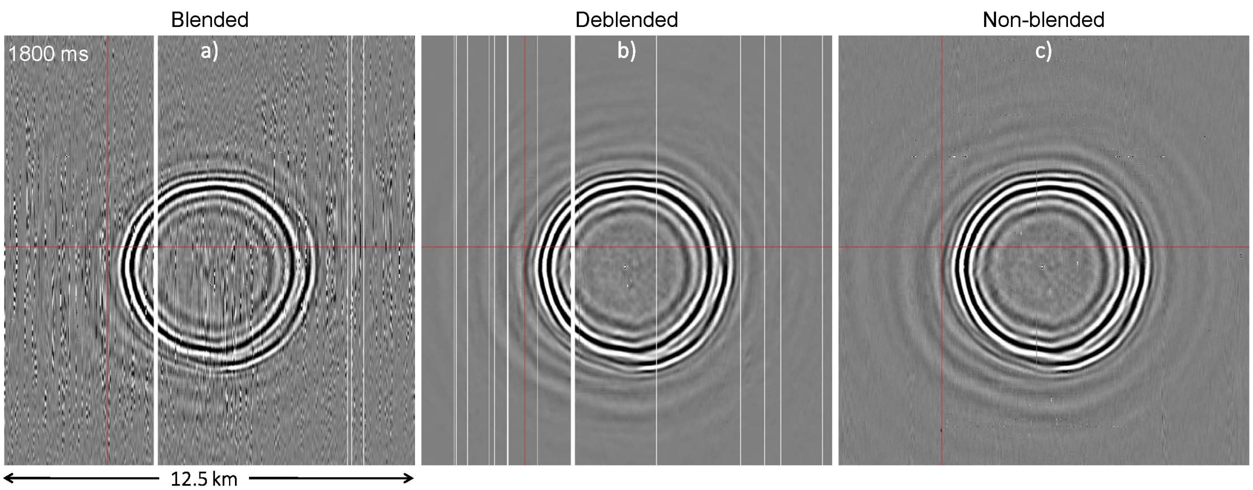

Figure 6: Cross-spread time slices at 1800 ms of the data shown in Figure 5 after 6 Hz high-cut filter: a) input data before deblending; b) deblended output; c) non-blended data representative of a perfect deblending result. (Data courtesy of Apache)

that our algorithm is equally effective in that setting.

CONCLUSIONS

A novel method of producing high-quality separation of blended seismic data has been presented. Its use has been demonstrated on OBN and land datasets. The method is inversion based, using an iterative thresholding scheme that allows the algorithm to effectively separate the blended signals. Our results on real data show that the algorithm performs exceptionally well recovering both the weaker and stronger parts of the wavefields.

ACKNOWLEDGEMENTS

We would like to thank AGS, Apache and DUG.

REFERENCES

Abma, R. L., 2010, Method for separating independent simultaneous sources: U.S. Patent 2010/003984.

Akerberg, P., G. Hampson, J. Rickett, H. Martin, and J. Cole, 2008, Simultaneous source separation by sparse Radon transform: 78th Annual International Meeting, SEG, Expanded Abstracts, 2801–2805.

Beasley, C. J., B. Dragoset, and A. Salama, 2012, A 3D simultaneous source field test processed using alternating projections: A new active separation method: Geophysical Prospecting, **60**, 591–601.

Berkhout, A. G., 2008, Changing the mindset in seismic data acquisition: The Leading Edge, **27**, 924–938, doi: https://doi.org/10.1190/1.2954035.

Hampson, G., J. Stefani, and F. Herkenhoff, 2008, Acquisition using simultaneous sources: The Leading Edge, **27**, 918–923, doi: https://doi.org/10.1190/1.3063930.

Kumar, A., G. Hampson, N. Vice, and T. Thompson, 2020, Inversion-based deblending using iterative thresholding: Accepted for Presentation at the 82nd EAGE Conference and Exhibition, European Association of Geoscientists and Engineers.

Mahdad, A., P. Doulgeris, and G. Blacquiere, 2011, Separation of blended data by iterative estimation and subtraction of blending interference noise: Geophysics, **76**, no. 3, Q9–Q17, doi: https://doi.org/10.1190/1.3556597.

Maraschini, M., A. Kielius, and S. Grion, 2016, Rank-reduction deblending for record length extension: The example of the Carnarvon basin: 86th Annual International Meeting, SEG, Expanded Abstracts, 4628–4632, doi: https://doi.org/10.1190/segam2016-13685251.1.

Moore, I., B. Dragoset, T. Ommundsen, D. Wilson, C. Ward, and D. Eke, 2008, Simultaneous source separation using dithered sources: 78th Annual International Meeting, SEG, Expanded Abstracts, 2806–2810, doi: https://doi.org/10.1190/1.3063928.

Trickett, S., L. Burroughs, and A. Milton, 2012, Robust rank-reduction filtering for erratic noise: 82th Annual International Meeting, SEG, Expanded Abstracts, 1–5, doi: https://doi.org/10.1190/segam2012-0129.1.

van Borselen, R., R. Baardman, T. Martin, B. Goswami, and E. Fromyr, 2012, An inversion approach to separating sources in marine simultaneous shooting acquisition — Application to a Gulf of Mexico data set: Geophysical Prospecting, **60**, 640–647, doi: https://doi.org/10.1111/j.1365-2478.2012.01076.x.

Yanchak, D., P. Aaron, A. Jaiswal, D. Monk, G. Wool, and M. Yates, 2019, An empirical assessment of deblending results on land vibroseis data: 89th Annual International Meeting, SEG, Expanded Abstracts, 4024–4028, doi: https://doi.org/10.1190/segam2019-3215045.1.